ORGANIC CHEMISTRY FRONTIERS

RESEARCH ARTICLE

View Article Online
View Journal | View Issue

Cite this: *Org. Chem. Front.*, 2026, **13**, 130

Synthesis of noradamantane building blocks

Matthew Todd,[a] Ivana Císařová,[b] Zdeněk Tošner[a] and Radim Hrdina *[a]

Received 12th August 2025,
Accepted 14th October 2025

DOI: 10.1039/d5qo01150g

rsc.li/frontiers-organic

The carbon scaffold of noradamantane, a ring contracted adamantane derivative, is notoriously difficult to selectively oxidise and functionalise, which limits the hydrocarbon's use as a building block for preparing noradamantyl decorated targets. In this research we disclose the use of Burgess reagent in a ring-contraction of pre-functionalised 2-amino-adamantan-1-ols to noradamantyl carbaldehydes in a pinacol-type rearrangement, that can be readily post-functionalised and further derivatised. To showcase their potential applicability, we performed structural analysis and their comparison to *ortho*- and *meta*-substituted benzene together with the synthesis of bioisosteric analogues of known drug molecules. We also report a new C12 parent cage hydrocarbon that was prepared by the same method from a diamantane precursor. This work may prompt further implementation of noradamantane as a sacffold for new molecular frameworks and help recognizing its utility in the space of chemical synthesis.

Introduction

Adamantane, dubbed the "lipophilic bullet",[1] can be regarded as one of the cornerstone representatives of the cage hydrocarbon family with its unique reactivity, that arises from its tight and symmetrical cage,[2–4] that has been broadly applied throughout the years in catalysis,[5,6] material science[7,8] and drug design.[1,9] Noradamantane, however, is in stark contrast to adamantane. The added strain leads to diminished reactivity, making selective oxidation of its cage difficult and access to its substituted derivatives fairly limited.[10] These difficulties were made clear shortly after its parent hydrocarbon synthesis in the 1960's,[11] thus prompting researchers to find alternative ways around its poor reactivity to prepare poly-substituted derivatives. Known methods for the preparation rely on dissolving-metal reduction[12] or cascade condensations[13] of unsaturated bicyclic precursors or radical cleavage of the adamantane framework followed by a ring closure (Fig. 1C).[14] One of the most recent approaches are based on triflic acid promoted decarboxylation of annulated adamantyl carbamates (Fig. 1C).[15] The liberated amine, unable to close an aziridine ring, drives the pinacol-type rearrangement of the adjacent C–C bond to the generated carbocation, contracting the scaffold. Reduction or hydrolysis of the resulting imine yields either aminomethyl-[16] or formyl-substituted noradamantanes respectively.[15] The main drawbacks of the previously mentioned methods are the limited access to starting materials (namely substituted adamantan-2-ones) and fairly harsh conditions that narrowed the scope to simple alkyl fragments.[15,16] As a result, mainly mono-substituted noradamantane derivatives have found their use as terminal building blocks (Fig. 1B).[17,18] Its poly-substituted derivatives could serve as conformationally locked, saturated and rigid linkers, when contemplating about their use in chemical synthesis. 1,3- and 3,7-disubstituted noradamantane derivatives could also serve as

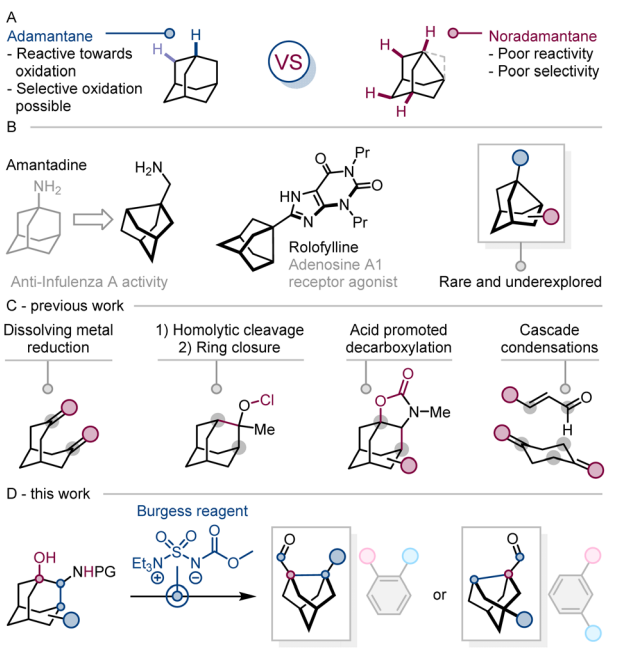

Fig. 1 (A) Reactivity of adamantane and noradamantane. (B) Current applications. (C) Previous methods for noradamantane preparation. (D) This work.

[a]*Charles University, Faculty of Science, Department of Organic Chemistry, Hlavova 8, 12840 Praha, Czech Republic. E-mail: radim.hrdina@natur.cuni.cz*
[b]*Charles University, Faculty of Science, Department of Inorganic Chemistry, Hlavova 8, 12840 Praha, Czech Republic*

isosters of the *ortho*- and *meta*-substituted phenyl ring.[19,20] Herein, we report on our newly developed method for the simultaneous preparation of 1,3- and 3,7-disubstituted noradamantane carbaldehydes, their structural analysis and post-functionalisation (Fig. 1D).

Results and discussion

Building upon previous knowledge, we sought to overcome the main limitations by executing the pinacol-type rearrangement from 2-aminoadamantan-1-ols,[21,22] that can be obtained by hydrolysis of the annulated carbamates,[23] as the free hydroxyl group could be transformed into a better leaving group and carbocation surrogate.[15,16] As aforementioned, starting materials of this nature aren't commercially available and were synthesized according to established procedures (Scheme 1A).[15,24,25]

Synthesis of starting materials

The main challenge was to carry the functional groups (or their masked surrogates) throughout the synthesis without their interference *via* unwanted side reactions. The annulated carbamates were synthesized by methods: (A) rhodium catalysed C–H amination of carbamate precursors;[25] (B) thermal decomposition of azidocarbonates[15,24] followed by basic hydrolysis to afford the 1,2-amino-alcohol derivatives (Scheme 1A). To introduce an oxygen containing functional group, benzyl ethers **4c–f** were prepared by method A, as method B led to ring opening or debenzylation of the starting materials and overall poor yields. Attempts to incorporate a nitrogen functional group as amides or carbamates caused ring opening side reactions, mainly during hydrolysis steps. Thus, the nitro-group was employed as an amine surrogate, that could be reduced later-on.[26] The corresponding nitro-derivatives **4g–i** where prepared by method B, as method A failed during the C–H amination step, possibly due to coordination to the rhodium catalyst, inhibiting its activity. The thermally generated nitrene produced the distal regio-isomer **4h** in a ratio of 10 : 1 to the proximal regio-isomer **4g**. This could be caused by strong deactivation of the secondary C–H bonds between the two substituted bridgehead positions. Attempts to change the ratio by UV decomposition of the azide precursor (254 nm lamp) or by using Sukbok Chang's cobalt catalyst[27] were unsuccessful (see SI page 41 and 42). Due to only small amounts of isomer **4g** produced, only the distal isomer **4h** was carried to the next steps. The diamantane amino alcohol **4j** was prepared by method B as an inseparable mixture of regio- and diastereo-isomers (Scheme 1B).

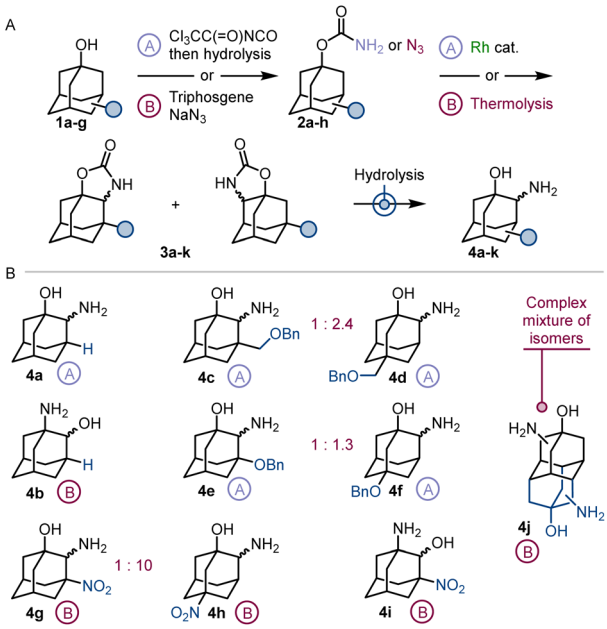

Scheme 1 A) General methods for the synthesis of 2-amino-adamantan-1-ols. (B) Table of prepared 2-amino-adamantan-1-ols.

Ring-contraction development

With a series of adamantane 1,2-amino-alcohols in hand, we searched for reaction conditions using the unsubstituted 2-aminoadamantan-1-ol **4a** as the model substrate. The reagent of choice was the inexpensive Burgess reagent (Scheme 2A).[28,29]

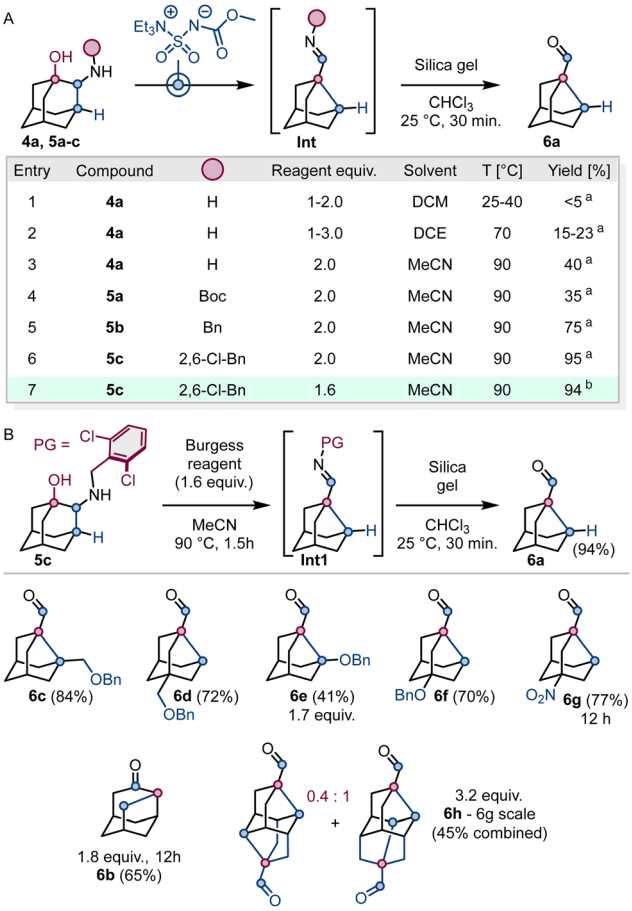

Entry	Compound		Reagent equiv.	Solvent	T [°C]	Yield [%]
1	**4a**	H	1-2.0	DCM	25-40	<5 [a]
2	**4a**	H	1-3.0	DCE	70	15-23 [a]
3	**4a**	H	2.0	MeCN	90	40 [a]
4	**5a**	Boc	2.0	MeCN	90	35 [a]
5	**5b**	Bn	2.0	MeCN	90	75 [a]
6	**5c**	2,6-Cl-Bn	2.0	MeCN	90	95 [a]
7	**5c**	2,6-Cl-Bn	1.6	MeCN	90	94 [b]

Scheme 2 A) Optimisation of reaction conditions with Burgess reagent. [a] NMR conversion, [b] yield of isolated comp. (B) Optimised conditions and substrate scope (yields of isolated compounds).

Initial attempts at lower temperature produced only trace amounts of the desired product **6a** (Scheme 2A; entry 1). The yield peaked at 40% when increasing the temperature to 90 °C (entry 3). The low yield was attributed to the secondary amine being the superior nucleophile that consumes the reagent. Protection of the amine with an electron-withdrawing group (**5a**) decreased the yield to 35% (entry 4). The *N*-benzylated amine **5b** improved the yield significantly to 75% (entry 5). 2,6-Dichlorobenzyl protected amine **5c** pushed the yield to 95% (entry 6), presumably due to added steric hindrance. In the final conditions the Burgess reagent loading decreased to 1.6 equivalents with **6a** isolated in a yield of 94% on a 0.5 g scale (entry 7). The imine **Int1** was not isolated but hydrolysed to carbaldehyde with silica gel in reagent-grade chloroform. The resulting slurry was filtered through a pad of silica gel and the carbaldehyde eluted with pure chloroform (Scheme 2). The rest of the 1,2-amino-alcohol derivatives were *N*-protected in high yields (>80%) and the scope of the reaction explored (Scheme 2B). Methylene ethers **5e** and **5f** underwent smooth rearrangement to carbaldehydes **6c** and **6d** in 84% and 72% yields respectively. Substrates with heteroatoms placed directly on the adamantane cage behaved more unpredictably. Unsymmetrical benzylated alcohol **5h** rearranged in a relatively high yield of 70% (**6f**). Interestingly, its symmetrical counterpart **5g** provided the carbaldehyde **6e** in only 41% yield accompanied by a complex mixture of side products. The nitro-derivative **5i** required a longer reaction time to fully convert to carbaldehyde **6g** and was obtained in 77% yield. The reaction of the inverted amino-alcohol **5d** produced protoadamantan-2-one (**6b**) in 65% yield, inferior to other published methods,[30] requiring a longer reaction time and a higher reagent loading. At last, we were pleased to see that the diamantane starting material **5j** successfully underwent the double contraction of its scaffold affording a 0.4 : 1 mixture of carbaldehydes **6h** in a combined yield of 45% on a 6 g scale, where the formation of the symmetrical aldehyde was not observed by previous methods (Scheme 2B).[15] It is important to note, that from a practical stand-point, one can carry the mixture of annulated carbamate precursors (Scheme 1 **3a–k**) to the final step without individual separation (only minor purification), as the regio-isomers are easily separable before (as **5c–j**) or after the rearrangement reaction (**6a–f**)(Scheme 2B).

We also wanted to explore the possibility of rearranging amino-alcohol **4b** to aldehyde **6a** *via* a deamination (Tiffeneau–Demjanov) reaction that is used for the synthesis of protoadamantan-2-one **6b** (Scheme 3).[30] The original aqueous conditions resulted in poor conversion, low yield of carbaldehyde **6a** and a mixture of side products (Scheme 3A; entry 1). Varying the Brønsted acid gave negative results with only trace amounts of product observed in NMR together with the unreacted starting material (entry 2). Moving from aqueous to organic solvents required the use of organic solvent soluble iso-amyl nitrite (iAm-ONO) as the diazotation reagent. At low temperature only trace product formation was observed by NMR accompanied by unreacted starting material (entry 3). Increasing the temperature greatly improved the yield of

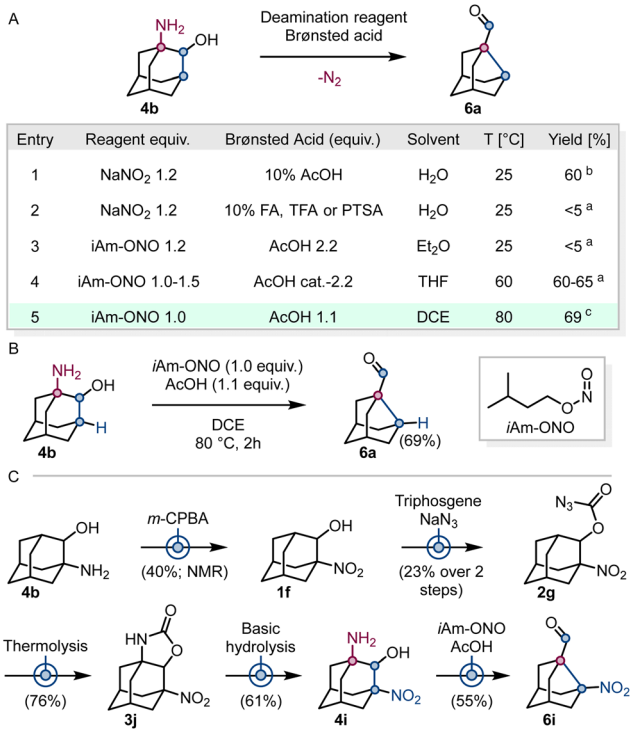

Entry	Reagent equiv.	Brønsted Acid (equiv.)	Solvent	T [°C]	Yield [%]
1	$NaNO_2$ 1.2	10% AcOH	H_2O	25	60 [b]
2	$NaNO_2$ 1.2	10% FA, TFA or PTSA	H_2O	25	<5 [a]
3	iAm-ONO 1.2	AcOH 2.2	Et_2O	25	<5 [a]
4	iAm-ONO 1.0-1.5	AcOH cat.-2.2	THF	60	60-65 [a]
5	iAm-ONO 1.0	AcOH 1.1	DCE	80	69 [c]

Scheme 3 A) Optimisation of deaminative conditions. [a] NMR yield, [b] conversion, [c] isolated yield (B) optimised reaction conditions. (C) Synthetic route to nitro-carbaldehyde **6i**.

product **6a**. Varying the equivalents of iAm-ONO and AcOH had no significant effect with yields remaining from 60 to 65% (entry 4). Further increase in temperature gave only a minor improvement pushing the isolated yield of aldehyde **6a** to 69% (Scheme 3B). With new conditions in hand we wanted to make up for the un-obtained nitro-aldehyde **6i** (Scheme 3C). Starting from amino-alcohol **4b** the oxidation of the amine gave nitro-alcohol **1f** in 40% (NMR) yield that proved to be difficult to isolate and was carried to the next step without purification (Scheme 5). The azide **2g** was therefore obtained in a 23% yield over two steps. Thermally initiated C–H amination followed by hydrolysis gave the desired nitro-amino-alcohol **4i** that successfully rearranged to the nitro-aldehyde **6i** in 55% yield (Scheme 3C).

Postfunctionalisation

An advantage of the reaction products is the versatility of the carbaldehyde functional group, allowing for oxidative or reductive transformations such as Jones oxidation, hydride reduction or reductive amination to afford corresponding carboxylic acids, methylene alcohols and amines respectively. The protected or masked functional groups also allow for convenient desymmetrisation for further derivatisation. Deprotection of benzyl ethers or reduction of the nitro-group with an H_2 balloon over Pd/C, together with previously mentioned transformations, proceed without the ring expansion back to adamantane. Reactions involving radical processes are

also feasible, as demonstrated on a nickel-catalysed decarboxylative Giese reaction of **13c** with *tert*-butyl acrylate, giving ester **15** in 65% yield (Scheme 4A).[31]

Regarding the products of the diamantane contraction (Scheme 4B), the mixture of carbaldehydes **6h** turned out to be inseparable by conventional separation techniques. Luckily, reduction with methanolic sodium borohydride allowed the individual separation of methylene alcohols **7c** and **7d** and confirmation of their structures with X-ray crystallography. To our best knowledge, the parent hydrocarbons of these derivatives had not been fully isolated and characterized.[32] Thus, we took the challenge of their synthesis. Jones oxidation converted alcohols **7c** and **7d** to carboxylic acids **8g** and **8h**. Decarboxylation attempts with both thermally and UV promoted Barton decarboxylation[33] or a photochemical iron-catalysed decarboxylation[34] gave only trace amounts of the desired products (see SI page 43–45). A nickel catalysed decarboxylation procedure[31] of redox-active esters **13a** and **13b** produced the hydrocarbons in isolable yields after eluting the crude mixture through a short pentane silica gel column. Interestingly, derivatives of the unsymmetrical scaffold (**7d**, **8h** and **13b**) were well soluble in most organic solvents when compared to the symmetrical scaffold (**7c**, **8g** and **13a**) that exhibited extremely poor solubility, making any manipulation fairly difficult. Nonetheless, we managed to crystallize hydrocarbon **14a** and confirm its structure by X-ray crystallography (Scheme 4D).

Structural analysis

We then took on the task of analysis and comparison of the synthesized products (Scheme 4C). Both 3,7- and 1,3-disubstitued noradamantane derivatives **9a** and **9b** were compared to *ortho*- and *meta*-substituted benzene **9a′** and **9b′**. The structures were computed using the Orca 6.0 software package.[35] The C–C bond length of the symmetrical diol **9a** bridge is, as expected, longer at 1.60 Å compared to the 1.40 Å of *ortho*-substituted benzene **9a′**. However, its substituent exit vector is slightly shallower at 118° setting the two methylene carbons the same distance of 3.0 Å apart. As for the un-symmetrical diol **9b**, the distance of 2.38 Å between the two quaternary carbon atoms almost matches the case of *meta*-substituted benzene **9b′** at 2.42 Å. Substituent exit vector angles vary at 148° and 153°, most likely due to the slightly different hybridization of the carbon atoms, but balance out, setting the two methylene carbons 5.0 Å away from each other, matching its benzene counterpart. The different substituent positions introduce a torsion angle of 26° along a virtual bond between the quaternary carbons. An overlay of the structures shows a high degree of similarity, when replacing both *ortho*- and *meta*-phenyls with di-substituted noradamantanes (Scheme 4C). The rod-shaped diamantane-derived compounds (**7c** and **7d**) can be envisioned as linear and rigid linkers or spacers that could be used in material science or as guests in macrocyclic molecules such as cyclodextrins or cucurbiturils (Scheme 4D).[36] The symmetrical diol **7c** separates both hydroxy-methylene substituents 6.68 Å apart with a dihedral angle of 180° and an exit vector angle of 156°, relative to its centre axis. Its elongated C–C bonds of 1.60 Å correspond to the computed values for noradamantane diol **9a**. The unsymmetrical diol **7d** spans the distance of 6.28 Å between the methylene carbon atoms with a torsion value of 51° and exit vector angles of 147°, also relative to its centre axis. Buckling the cage in the same direction shortened the previously longer bonds to 1.57 Å. As for the parent hydrocarbon **14a**, its height was measured to be 3.78 Å. The central cyclohexyl belt is puckered, stretched to 3.00 Å in the direction of the elongated bonds and contracted in the perpendicular direction to 2.63 Å (Scheme 4D).

Synthesis of drug analogues

Following the structural assessment, we synthesized analogues of drug molecules containing the disubstituted noradamantane core to demonstrate potential applicability. First idea was to mimic modified nucleosides, that are used in the development of antiviral agents, that often modify or replace the central sugar fragment,[37] such as Abacavir (**11c′**) (Scheme 4E).[38,39] Reduction of benzyl ether **6e** followed by a Mitsunobu reaction with chloro-amino-purine gave product **11a** in excellent 70% yield. Nucleophilic displacement of the chlorine with excess of sodium azide in DMF gave **11b** in 86% yield. A final hydrogenation over palladised charcoal reduced the azide and cleaved the benzyl protecting group, successfully affording the modified nucleoside mimic **11c** in a yield of 89%. Overlay of the mimic **11c** (grey) and Abacavir **11c′** (violet, transparent) shows similarity in the spatial disposition and distances between the key functional groups and fragments. The two substituted carbons of the cyclopentene (**11c′**) ring span a distance of 2.48 Å, whereas the noradamantane derivative **11c** sets the substituents 2.71 Å apart (Scheme 4E). Phthalylsulfathiazole **12b′**, an antimicrobial drug,[40,41] was chosen as our next target, replacing the *ortho*-substituted benzene ring with 3,7-di-substituted noradamantane (Scheme 4F). Oxidation of diol **9a** with aqueous $KMnO_4$ gave the carboxylic acid **12a** in 73% yield. Reaction of **12a** with EDC·HCl and DMAP afforded the corresponding anhydride **12a′** that was carried over without isolation. Refluxing the anhydride **12a′** in anhydrous MeCN with inexpensive and commercially available sulfathiazole in the presence of Et_3N and DMAP produced the desired analogue **12b** in a 57% yield without column chromatography. The bridge C–C bond of **12b** is slightly stretched to 1.61 Å, shallowing the exit vector angle and shortening the distance of the carbonyl carbons to 2.93 Å, compared to 3.06 Å for **12b′** with the phenyl ring carbons, remaining at 1.40 Å apart. Overlay of **12b** (grey) and **12b′** (violet, transparent) shows near perfect overlap of the noradamantane bioisostere **12b** with the phthalylsulfathiazole (**12b′**) phenyl ring (Scheme 4F).

Mechanistic investigation

In contrast to the ring-expansion of noradamantane back to adamantane,[42,43] mechanistic studies of the contraction to noradamantane have been conducted only recently.[15] The reaction is proposed to be driven by the difference in the thermodynamic stability of the formed bridgehead carbocation and

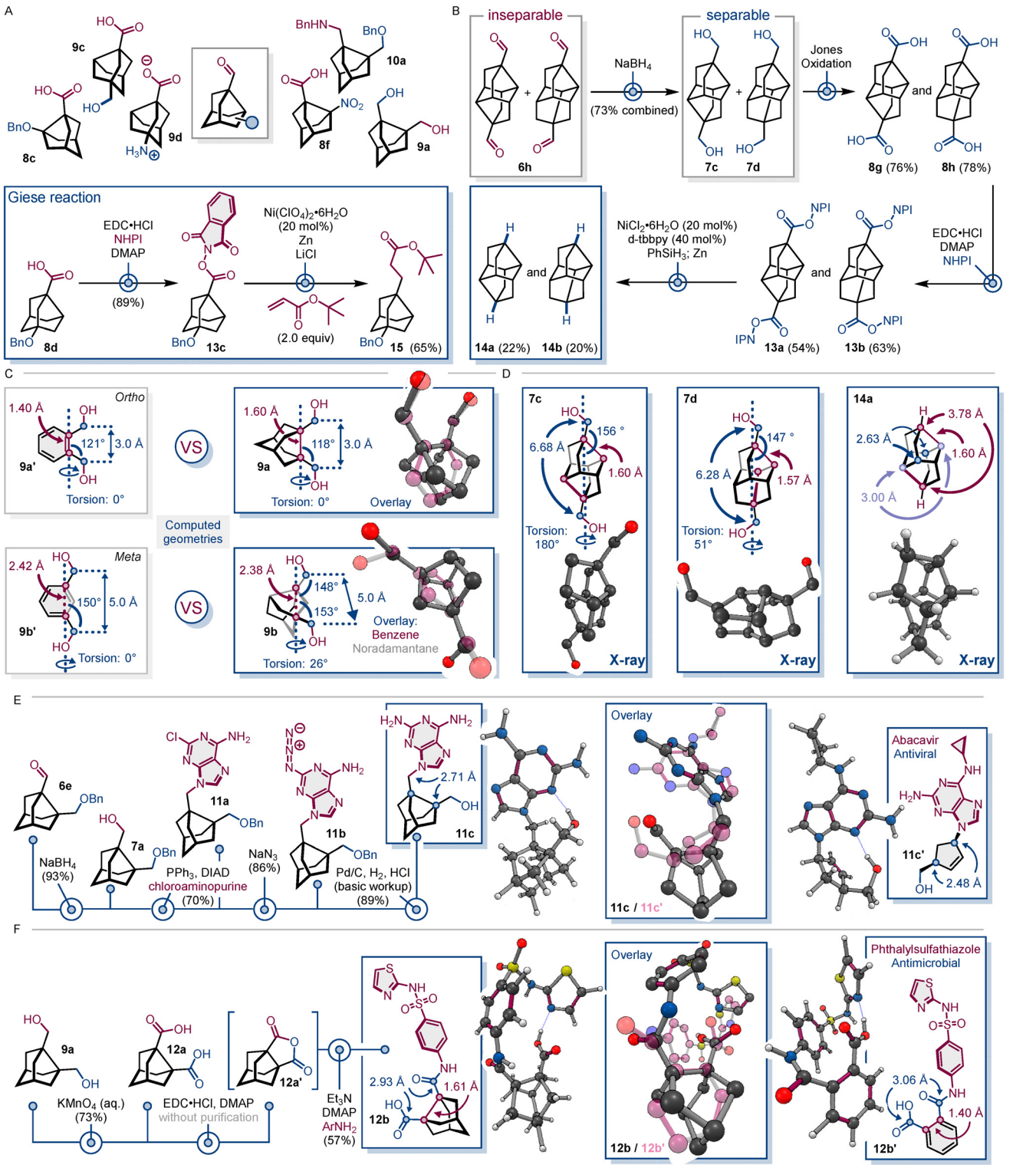

Scheme 4 A) Postfunctionalisation of noradamantane carbaldehydes. (B) Synthesis of parent hydrocarbons **14a** and **14b**. (C) Structural analysis and comparison of noradamantane carbaldehydes **9a** and **9b** with *ortho*-(**9a'**) and *meta*-substituted (**9b'**) benzene rings. (D) Structural analysis of diamantane derived compounds **7c**, **7d** and **14a**. (E) Synthesis of antiviral analogue **11c**. (F) Synthesis of antifungal analogue **12b**.

the rearranged *N*-methylated iminium salt, calculated to be approximately 22 kcal mol^{-1}, where the rate determining step (RDS) is the formation of the bridgehead carbocation. The 1,2-alkyl shift was calculated to have a shallow barrier of 0.79 kcal mol^{-1}. The impact of additional functional groups on the rearrangement hasn't been explored so far (Scheme 5A).

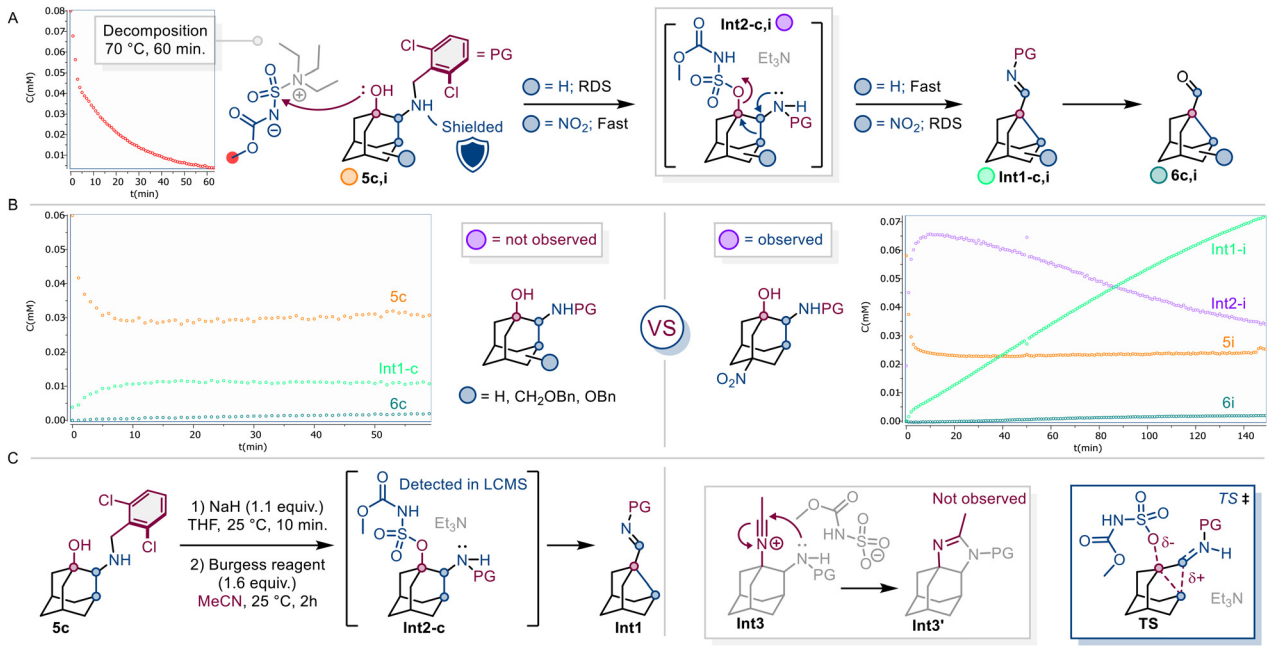

Scheme 5 A) Proposed reaction pathway. NMR measurement of Burgess reagent decomposition. (B) NMR kinetic studies of **5c** and **5i**. (C) Control experiment with sequential addition of sodium hydride and Burgess reagent.

The Burgess reagent is known to be thermally unstable.[44] Our case is no exception, as the reagent undergoes complete decomposition at 70 °C within 60 minutes (measured by NMR) (Scheme 5A). To gain deeper understanding of the individual reaction steps, we conducted NMR kinetic measurements at different temperatures. In the case of the simple amino-alcohol substrate **5c** the RDS turned out to be the nucleophilic substitution of the substrate with Burgess reagent followed by immediate imine (**Int1-c**) formation. The proposed sulfamidate intermediate **Int2-c** could not be observed. The reaction proceeds until the complete consumption/decomposition of Burgess reagent. The competition of the RDS and reagent decomposition would account for the necessity of excess reagent loading to reach full conversion of the starting material **5c** (Scheme 5B). As apparent from Scheme 2, most of the substrates, bearing substituents bound closer or further from the migrating C–C bond, underwent the transformation at the same rate except for nitro-derivative **5i** and inverted amino alcohol **5d**. When monitoring the reaction progress of nitro-derivative **5i** by LCMS and NMR, the sulfamidate intermediate **Int2-i** was detected and could be observed, suggesting the reversed speed of the individual reaction steps (Scheme 5B). The initial nucleophilic substitution of the substrate with the reagent becomes faster, whereas the cleavage of the C–O bond to form the carbocation becomes the RDS. The rearrangement maintains a rather shallow barrier, with no side-products, resulting from external trapping of the carbocation, observed (**Int3**, **Int3′**). The barrier of the RDS is likely higher due to the strong electron-withdrawing character of the nitro-group, that diminishes the hyperconjugative stabilisation of the forming positive charge, characteristic to adamantyl cation systems.[2,3]

We then performed a control experiment, where deprotonation of amino alcohol **5c** would form the more nucleophilic alkoxide, compared to the neutral alcohol, that would undergo the addition faster (Scheme 5C). Treatment of **5c** with NaH followed by Burgess reagent, evaporation and measurement of the crude mixture with NMR resulted in complete conversion and a 67% combined yield of the imine (**Int1**) and aldehyde (**6a**) products. The sulfamidate intermediate **Int2-c** could only be detected with LCMS of the crude reaction mixture, suggesting the fast nature of the rearrangement step (see SI page 47 and 51–58). Combined with the absence of side-products from solvent attack (**Int3**, **Int3′**), it can be suggested, that the 1,2-alkyl shift proceeds through a concerted transition state with a high degree of S_N2-like behaviour (**TS**).

Conclusion

In conclusion, we've developed a new method for the preparation of previously hard to obtain 1,3- and 3,7-di-substituted noradamantane building blocks from their corresponding adamantane precursors together with new functionalized C12 caged hydrocarbons, including their parent hydrocarbons, derived from diamantane. Structural analysis of the products and representative analogues of drug molecules containing the noradamantyl scaffold showed remarkable similarities with their phenyl containing counterparts. At last, we briefly investigated the impact of additional substituents on the nature of

the rearrangement. These results could motivate their application as isosteres of both *ortho*- and *meta*-substituted benzene in medicinal chemistry or as rigid spacers/linkers with defined angles and distances in catalysis and material design, increasing the poor recognition of the noradamantane scaffold in the current environment of chemical synthesis.

Author contributions

M. T.: developed and optimised the reaction, explored the substrate scope, showcased further transformations and applications, computed the structures and wrote the manuscript and SI; I. C.: performed X-ray crystallography; Z. T.: performed NMR measurements and R. H.: supervised the project.

Conflicts of interest

There are no conflicts to declare.

Data availability

Supplementary information (SI): experimental procedures, compounds descriptions, X-ray data and copies of NMR spectra. See DOI: **https://doi.org/10.1039/d5qo01150g**.

CCDC 2441791–2441793 contain the supplementary crystallographic data for this paper.[45a–c]

Acknowledgements

Computational resources were provided by the e-INFRA CZ project (ID: 90254) supported by the Ministry of Education, Youth and Sports of the Czech Republic. We also thank Dr Štícha and Dr Urban from Charles University for HRMS and IR measurements.

References

1 L. Wanka, K. Iqbal and P. R. Schreiner, The Lipophilic Bullet Hits the Targets: Medicinal Chemistry of Adamantane Derivatives, *Chem. Rev.*, 2013, **113**, 3516–3604.
2 R. C. Fort and P. von R. Schleyer, Adamantane: Consequences of the Diamondoid Structure, *Chem. Rev.*, 1964, **64**, 277–300.
3 J. I.-C. Wu and P. von R. Schleyer, Hyperconjugation in hydrocarbons: Not just a "mild sort of conjugation", *Pure Appl. Chem.*, 2013, **85**, 921–940.
4 A. A. Fokin and P. R. Schreiner, in *Strategies and Tactics in Organic Synthesis*, ed. M. Harmata, Academic Press, 2012, vol. 8, pp. 317–350.
5 K. A. Agnew-Francis and C. M. Williams, Catalysts Containing the Adamantane Scaffold, *Adv. Synth. Catal.*, 2016, **358**, 675–700.
6 R. C. Wende and P. R. Schreiner, Evolution of asymmetric organocatalysis: multi- and retrocatalysis, *Green Chem.*, 2012, **14**, 1821–1849.
7 H. Nasrallah and J.-C. Hierso, Porous materials based on 3-dimensional Td-directing functionalized adamantane scaffolds and applied as recyclable catalysts, *Chem. Mater.*, 2019, **31**, 619–642.
8 T. Muller and S. Bräse, Tetrahedral organic molecules as components in supramolecular architectures and in covalent assemblies, networks and polymers, *RSC Adv.*, 2014, **4**, 6886–6907.
9 C. Dane, A. P. Montgomery and M. Kassiou, The adamantane scaffold: Beyond a lipophilic moiety, *Eur. J. Med. Chem.*, 2025, **291**, 117592.
10 J. S. Wishnok, P. v. R. Schleyer, E. Funke, G. D. Pandit, R. O. Williams and A. Nickon, Syntheses in the noradamantane series, *J. Org. Chem.*, 1973, **38**, 539–542.
11 B. R. Vogt and J. R. E. Hoover, The Synthesis of Noradamantane, *Tetrahedron Lett.*, 1967, **8**, 2841–2843.
12 M. Eakin, J. Martin and W. Parker, Transannular reactions in the bicyclo[3,3,1]nonane system, *Chem. Commun.*, 1965, 206a.
13 K. Daskalakis, N. Umekubo, S. Indu, G. Kawauchi, T. Taniguchi, K. Monde and Y. Hayashi, Asymmetric Synthesis of Noradamantane Scaffolds via Diphenylprolinol Silyl Ether-Mediated Domino Michael/Epimerization/Michael (or Aldol)/1,2-Addition Reactions, *Angew. Chem., Int. Ed.*, 2025, **64**, e202500378.
14 R. M. Black and G. B. Gill, The cleavage of t-adamantyloxy-radicals, *J. Chem. Soc. D*, 1970, 972–973.
15 B. Zonker, J. Becker and R. Hrdina, Synthesis of noradamantane derivatives by ring-contraction of the adamantane framework, *Org. Biomol. Chem.*, 2021, **19**, 4027–4031.
16 R. Hrdina, O. M. Holovko-Kamoshenkova, I. Císařová, F. Koucký and O. Machalický, Annulated carbamates are precursors for the ring contraction of the adamantane framework, *RSC Adv.*, 2022, **12**, 31056–31060.
17 B. Gopalan, T. Ponpandian, V. Kachhadia, K. Bharathimohan, R. Vignesh, V. Sivasudar, S. Narayanan, B. Mandar, R. Praveen, N. Saranya, S. Rajagopal and S. Rajagopal, Discovery of adamantane based highly potent HDAC inhibitors, *Bioorg. Med. Chem. Lett.*, 2013, **23**, 2532–2537.
18 S. Codony, E. Valverde, R. Leiva, J. Brea, M. Isabel Loza, C. Morisseau, B. D. Hammock and S. Vázquez, Exploring the size of the lipophilic unit of the soluble epoxide hydrolase inhibitors, *Bioorg. Med. Chem.*, 2019, **27**, 115078.
19 J. Tsien, C. Hu, R. R. Merchant and T. Qin, Three-dimensional saturated C(sp3)-rich bioisosteres for benzene, *Nat. Rev. Chem.*, 2024, **8**, 605–627.
20 M. A. M. Subbaiah and N. A. Meanwell, Bioisosteres of the phenyl ring: recent strategic applications in lead optimization and drug design, *J. Med. Chem.*, 2021, **64**, 14046–14128.
21 R. Hrdina, Directed C–H functionalization of the adamantane framework, *Synthesis*, 2019, 629–642.

22 M. Todd and R. Hrdina, Synthesis of 1, 2-Disubstituted Adamantane Derivatives by Construction of the Adamantane Framework, *Molecules*, 2023, **28**, 7636.
23 R. Hrdina, M. Larrosa and C. Logemann, Triflic Acid Promoted Decarboxylation of Adamantane-Oxazolidine-2-One: Access to Chiral Amines and Heterocycles, *J. Org. Chem.*, 2017, **82**, 4891–4899.
24 P. F. Alewood, M. Benn and R. Reinfried, Cyclizations of Azidoformates to Tetrahydro-1, 3-oxazin-2-ones and Oxazolidin-2-ones, *Can. J. Chem.*, 1974, **52**, 4083–4089.
25 J. J. Rohde, M. A. Pliushchev, B. K. Sorensen, D. Wodka, Q. Shuai, J. Wang, S. Fung, K. M. Monzon, W. J. Chiou, L. Pan, X. Deng, L. E. Chovan, A. Ramaiya, M. Mullally, R. F. Henry, D. F. Stolarik, H. M. Imade, K. C. Marsh, D. W. A. Beno, T. A. Fey, B. A. Droz, M. E. Brune, H. S. Camp, H. L. Sham, E. U. Frevert, P. B. Jacobson and J. T. Link, Discovery and Metabolic Stabilization of Potent and Selective 2-Amino-N-(adamant-2-yl) Acetamide 11β-Hydroxysteroid Dehydrogenase Type 1 Inhibitors, *J. Med. Chem.*, 2007, **50**, 149–164.
26 H. Schwertfeger, C. Würtele and P. R. Schreiner, Synthesis of diamondoid nitro compounds from amines with m-chloroperbenzoic acid, *Synlett*, 2010, 493–495.
27 J. Lee, J. Lee, H. Jung, D. Kim, J. Park and S. Chang, Versatile Cp* Co(III)(LX) catalyst system for selective intramolecular C–H amidation reactions, *J. Am. Chem. Soc.*, 2020, **142**, 12324–12332.
28 E. M. Burgess, H. R. Penton and E. A. Taylor, Synthetic applications of N-carboalkoxysulfamate esters, *J. Am. Chem. Soc.*, 1970, **92**, 5224–5226.
29 S. Santra, Burgess Reagent: From Oblivion to Renaissance in Organic Synthesis, *Synlett*, 2009, 328–329.
30 J. R. Alford and M. A. McKervey, A synthesis of 4-protoadamantanone, *J. Chem. Soc. D*, 1970, 615–616.
31 T. Qin, L. R. Malins, J. T. Edwards, R. R. Merchant, A. J. E. Novak, J. Z. Zhong, R. B. Mills, M. Yan, C. Yuan, M. D. Eastgate and P. S. Baran, Nickel–catalyzed Barton decarboxylation and Giese reactions: a practical take on classic transforms, *Angew. Chem., Int. Ed.*, 2017, **56**, 260–265.
32 A. de Meijere, C.-H. Lee, M. A. Kuznetsov, D. V. Gusev, S. I. Kozhushkov, A. A. Fokin and P. R. Schreiner, Preparation and Reactivity of [D3d]–Octahedrane: The Most Stable (CH)12 Hydrocarbon, *Chem. – Eur. J.*, 2005, **11**, 6175–6184.
33 D. H. R. Barton, D. Crich and W. B. Motherwell, The invention of new radical chain reactions. Part VIII. Radical chemistry of thiohydroxamic esters; A new method for the generation of carbon radicals from carboxylic acids, *Tetrahedron*, 1985, **41**, 3901–3924.
34 Y.-C. Lu and J. G. West, Chemoselective Decarboxylative Protonation Enabled by Cooperative Earth-Abundant Element Catalysis, *Angew. Chem., Int. Ed.*, 2023, **62**, e202213055.
35 F. Neese, Software Update: The ORCA Program System—Version 6.0, *Wiley Interdiscip. Rev.:Comput. Mol. Sci.*, 2025, **15**, e70019.
36 Z. Liu, W. Lin and Y. Liu, Macrocyclic supramolecular assemblies based on hyaluronic acid and their biological applications, *Acc. Chem. Res.*, 2022, **55**, 3417–3429.
37 A. A. Zenchenko, M. S. Drenichev, I. A. Il'icheva and S. N. Mikhailov, Antiviral and antimicrobial nucleoside derivatives: structural features and mechanisms of action, *Mol. Biol.*, 2021, **55**, 786–812.
38 M. T. Crimmins and B. W. King, An Efficient Asymmetric Approach to Carbocyclic Nucleosides: Asymmetric Synthesis of 1592U89, a Potent Inhibitor of HIV Reverse Transcriptase, *J. Org. Chem.*, 1996, **61**, 4192–4193.
39 PubChem, Abacavir, **https://pubchem.ncbi.nlm.nih.gov/compound/441300**, (accessed 28 July 2025).
40 W. E. Askue, E. Tufts and V. Droughman, Phthalylsulfathiazole (Sulfathalidine) in the Treatment of Enterobiasis (Pinworm Infection), *J. Pediatr.*, 1954, **44**, 380–385.
41 PubChem, Phthalylsulfathiazole, **https://pubchem.ncbi.nlm.nih.gov/compound/4806**, (accessed 28 July 2025).
42 D. T. Stoelting and V. J. Shiner Jr., Solvolysis of 1-(3-noradamantyl)ethyl sulfonates, *J. Am. Chem. Soc.*, 1993, **115**, 1695–1705.
43 B. Zonker, E. Duman, H. Hausmann, J. Becker and R. Hrdina, [1,2]-Rearrangement of iminium salts provides access to heterocycles with adamantane scaffold, *Org. Biomol. Chem.*, 2020, **18**, 4941–4945.
44 T. A. Metcalf, R. Simionescu and T. Hudlický, Design of thermally stable versions of the burgess reagent: stability and reactivity study, *J. Org. Chem.*, 2010, **75**, 3447–3450.
45 (*a*) CCDC 2441791: Experimental Crystal Structure Determination, 2025, DOI: **10.5517/ccdc.csd.cc2mywgy**; (*b*) CCDC 2441792: Experimental Crystal Structure Determination, 2025, DOI: **10.5517/ccdc.csd.cc2mywhz**; (*c*) CCDC 2441793: Experimental Crystal Structure Determination, 2025, DOI: **10.5517/ccdc.csd.cc2mywj0**.